Encapsulation of film bulk acoustic resonator filters using a wafer-level microcap array

Chung-Hsien Lin[1], Ju-Mei Lu[2] and Weileun Fang[1]

[1] Power Mechanical Engineering Department, National Tsing Hua University,
Hsinchu, Taiwan
[2] Asia Pacific Microsystems, Inc., Hsinchu, Taiwan

E-mail: fang@pme.nthu.edu.tw

Abstract
A simple method of protecting film bulk acoustic resonator (FBAR) filters
by wafer-level packaging is proposed. This method employs a reliable
silicon microcap structure to encapsulate FBAR filters. Since only
conventional processes and facilities were required to accomplish this work,
it is a cost-effective way to package FBAR filters. The fabrication process
consists of three steps: cavity etching, wafer bonding and wafer singulation.
In this study, the design and fabrication processes are described in detail.
Moreover, a filter designed for personal communication systems (PCS)
transmitter band is measured to demonstrate the performance variation after
the microcap process. The fabrication results and measurement results have
ensured the effectiveness of this process.

(Some figures in this article are in colour only in the electronic version)

1. Introduction

Film bulk acoustic resonator (FBAR) filters are micromachined high-frequency filters for RF communication systems. Since FBAR filters have high power handling capability and good thermal stability, their applications have been gradually increased. The design and fabrication methods of FBAR filters are extensively discussed in many articles [1–3]. However, the packaging of microsystems is a very challenging task. It is well known that the moving parts of MEMS devices are fragile and sensitive to the environment [4, 5]. Thus, many wafer-bonding and packaging methods were developed to protect microsystem structures, such as eutectic bonding [6, 7] and adhesive bonding [8, 9]. Packaging becomes even more complicated when dealing with RF microsystems, because high-frequency effects must also be taken into consideration [10]. Therefore, the packaging of FBAR devices is still one primary consideration, since they operate in radio frequency and consist of an extremely sensitive membrane which is only a few microns thick.

A standard IC packaging process could damage FBAR devices in many ways. For example, the high-pressure water

spraying on the wafer during dicing breaks the thin membrane structure of a FBAR. Moreover, the evaporation or outgassing material from solvents during die attachment would adhere to the membrane surface and influence its resonance frequency, further changing the characteristics of FBAR filters. There exist various packaging methods for protecting FBAR filters. Figure 1(a) shows a microcapped FBAR with through-wafer interconnection [11, 12]. Figure 1(b) shows another type of microcap, which can be fabricated directly on the device chip using a surface micromachining technique [13]. In short, the microcap method [11–13] is regarded as the easiest way to protect the thin film resonance region of a FBAR. After that, the standard IC fabrication processes such as dicing and passivation can be directly employed to handle the suspended microsystem devices. Nevertheless, the microcap realized either by a lapped wafer with through-wafer interconnection or surface micromachining is fabricated and integrated using additional complicated processes. Figure 1(c) shows a method that does not use any protection on the front side of a FBAR chip, but flip chip on a LTCC substrate as a protection of the front side [14]. The resonance membrane is not properly protected by this approach, and can easily be damaged during
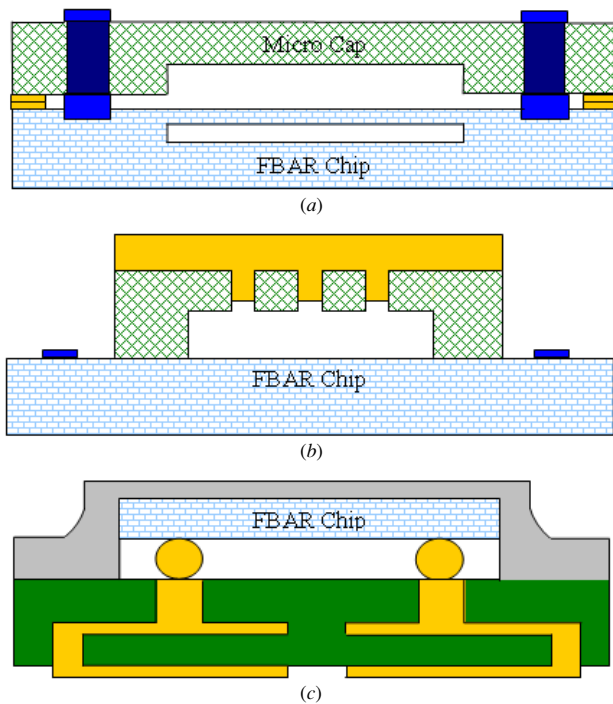
Figure 1. Schematic view of existing chip-scale packages for FBAR filters: (*a*) microcap with through-wafer interconnect, (*b*) photo-epoxy microcap, (*c*) flip chip on LTCC.

the packaging process. Hence, a simple yet reliable packaging process to encapsulate the thin film structure of a FBAR filter remains highly demanding.

This research presents a simple wafer-level packaging process to protect FBAR filters by using microcaps. The present packaging process has only three steps: bulk etching of a silicon wafer, eutectic or adhesive wafer bonding and singulation. These steps are very common for microfabrication. Therefore, this approach provides a promising way to package FBAR filters. Moreover, by using silicon microcaps, the fabricated FBAR filters have a stiff and reliable encapsulation structure.

2. Microcap process

The present process flow for the wafer-level packaging of FBAR filters is summarized in figure 2. First, a silicon wafer acting as the microcap was etched anisotropically to form cavities as shown in figure 2(*a*). The mesa in figure 2(*a*) performed as the spacer for the microcap and the FBAR. It prevented the contact of the microcap with the thin film membrane and the bonding pad. Thus the membrane is allowed to freely vibrate. Moreover, the spacer also prevented the bonding pad from being damaged by the following dicing process. Figure 2(*a*) also shows the top view of the mesa. The size of the etched cavity was $430 \times 860 \ \mu m^2$. The inner dimensions of the mesa rim around the cavity were $520 \times 970 \ \mu m^2$ and the outer dimensions of the rim were $990 \times 1390 \ \mu m^2$. The KOH solution was used to anisotropically etch cavities on the wafer, so as to form the mesa spacer. Since only 30 μm depth would be sufficient, the etching was accomplished in a short time of about 30 min. The
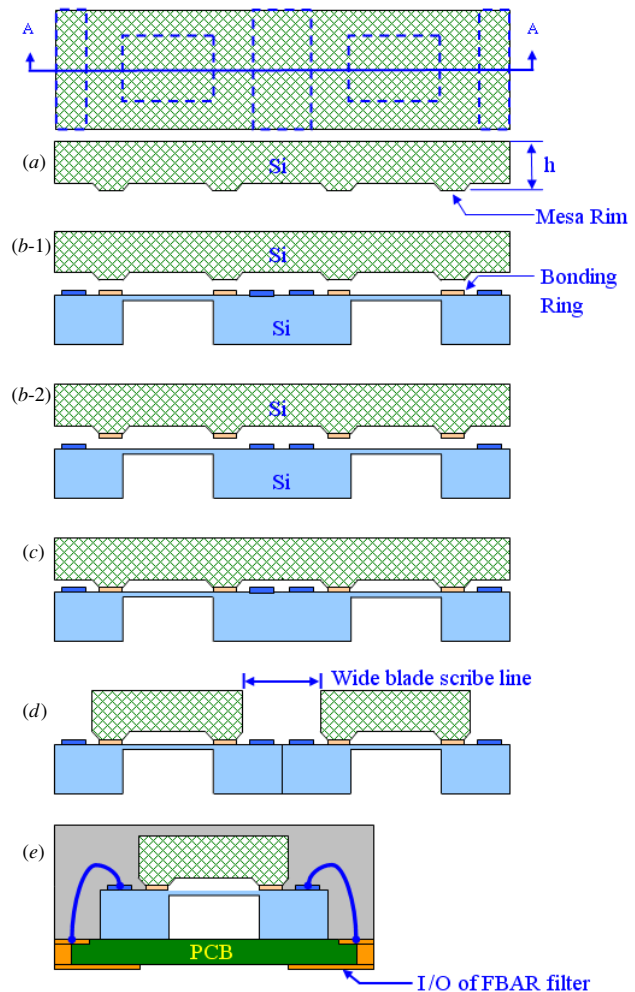
Figure 2. Process flow of the microcapped FBAR fabricated by the standard wafer saw method.

opposite side of the microcap wafer was also patterned by using a double-side aligner, since the following bonding and singulation processes required clear marks to better align wafers and define the scribe line area. Next, the wafer-bonding process was applied. Both eutectic and adhesive wafer-bonding techniques have been studied in this research. As shown in figure 2(*b*-1), the Au bonding ring was sputtered onto the device wafer for the eutectic-bonding process. On the other hand, the benzocyclobutene (BCB, an insulator) bonding ring was spun onto the cap wafer for the adhesive-bonding process, as shown in figure 2(*b*-2). The device wafer and cap wafer were then bonded by applying adequate pressure and temperature, as shown in figure 2(*c*). After that, a multi-step dicing was used to expose the bonding pad area and singulate each die after wafer bonding as shown in figure 2(*d*). Two different dicing blades were used to singulate the FBAR device. Firstly, the pads were exposed after vertical dicing by a wide blade of 750 μm kerf width, as indicated in figure 2(*d*). The dicing depth was determined by the thickness h of the silicon substrate in figure 2(*a*) to prevent the pads from being damaged. Moreover, it was necessary to employ a two-step dicing in the horizontal direction to fully separate the 800 μm thick bonded wafers. The thick (150 μm) kerf blade was used for the first cut, and the thin (30 μm) kerf blade was used for
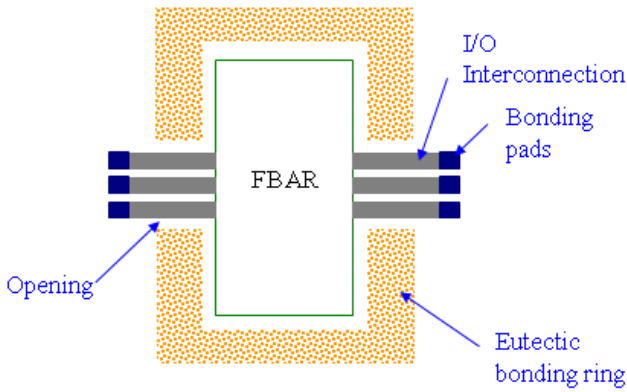
Figure 3. Schematic view of a eutectic bonding ring and interconnection lines.

the second cut. Finally, each FBAR device with its microcap was then singulated using a narrow blade of 30 μm kerf width. After the FBAR device was microcapped and singulated, it was packaged with standard wire-bonding and molding processes, as shown in figure 2(*e*).

There are several issues regarding eutectic and adhesive bondings which need to be further discussed. This study selected the Au–Si film as the material for eutectic bonding. The eutectic-bonding method has the advantage of low bonding temperature compared to fusion bonding and stable mechanical properties during the process. In addition, the eutectic-bonding method has a better thermal conductivity at the bonding interface. Therefore, the heat generated from the FBAR device can be easily dissipated through the interface to the microcap. As indicated in figure 2(*b*-1), the bonding ring was formed by a 1 μm thick Au film. The Au film was patterned to form a hollow square with two openings, as shown in figure 3. The inner square was 510×960 μm^2 and the outer square was 1000×1400 μm^2. The FBAR and bonding pad were connected by I/O interconnection. Since the Au film was conductive, the openings were employed to minimize interference. Finally, a cleaned silicon cap wafer was bonded onto the device wafer. The bonding temperature was near 450 °C, and a 3000 N force was applied to these two 6 inch wafers during bonding. Because there were about 4928 rings per wafer, the bonding pressure was about 670 kPa. The overall bonding process was under a vacuum environment at 10^{-1} bar, and took about 80 min.

As shown in figure 2(*b*-2), BCB was selected for the adhesive-bonding technique because of its low dielectric constant and high bonding strength as discussed in many literatures. The photosensitive BCB supplied by Dow Chemical Company was spun on the cap wafer and patterned into a hollow square shape by photolithography. The planar dimensions of the hollow square were the same as that of the eutectic bonding described previously (inner square was 510×960 μm^2 and the outer square was 1000×1400 μm^2). In addition, the thickness of the BCB was 10 μm. However, the openings for interconnection lines were no longer required in this case, because the BCB was dielectric. The SEM in figure 4(*a*) shows the cross section of the coated BCB ring. It is clearly observed that there is no residual BCB left inside the cavity after photolithography. In this case, a baking process at a temperature of 70 °C for 15 min was employed to drive out
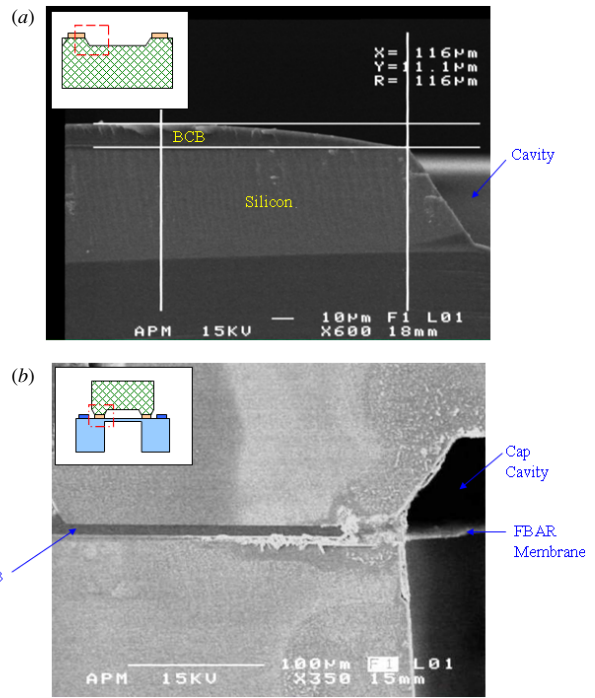

Figure 4. Cross-section SEM photo of a BCB bonding ring: (*a*) after photolithography, (*b*) after bonding.
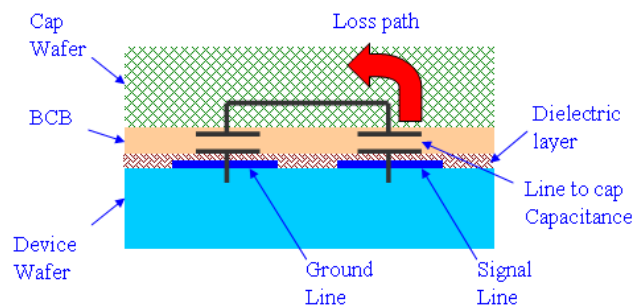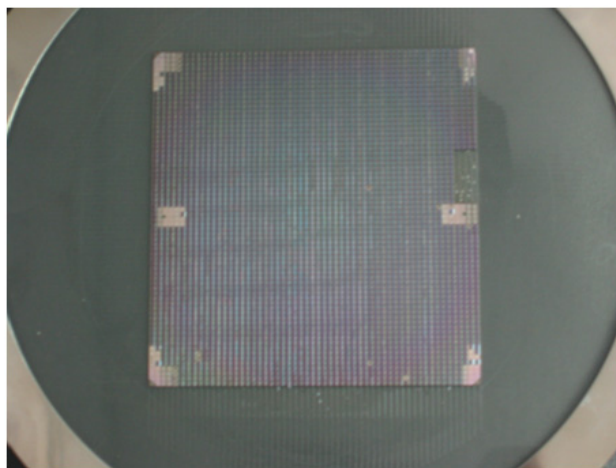

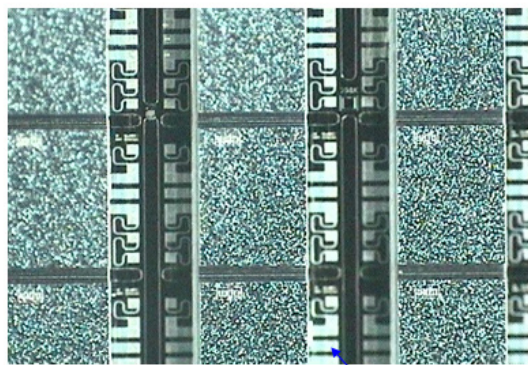**Figure 5.** RF signal leakage from signal lines into ground through the microcap.

solvents in the BCB solution before bonding. After that, the wafers were bonded inside a commercial bonding machine, and the curing process performed. The bonding conditions were at a temperature of 250 °C for 1.5 h, and a 3500 N bonding force was applied to the wafers. Figure 4(*b*) shows the cross section of a BCB bonding ring after bonding. As shown in the figure, the BCB did not fill the cap cavity during the bonding process. Although the thermal conductivity at the bonding interface was not as good as eutectic bonding, the insulator could better prevent RF signal leakage from signal lines into ground through the microcap, as shown in figure 5.

3. Experimental results

Typical fabrication results are shown in figure 6. Figure 6(*a*) shows the microcapped FBAR filters array after wafer-level packaging on a 6 inch substrate. The close-up photo in figure 6(*b*) shows that the bonding pads were not damaged during the multi-step dicing process. The close-up SEM photo in figure 7(*a*) clearly shows the scribe lines from both wide
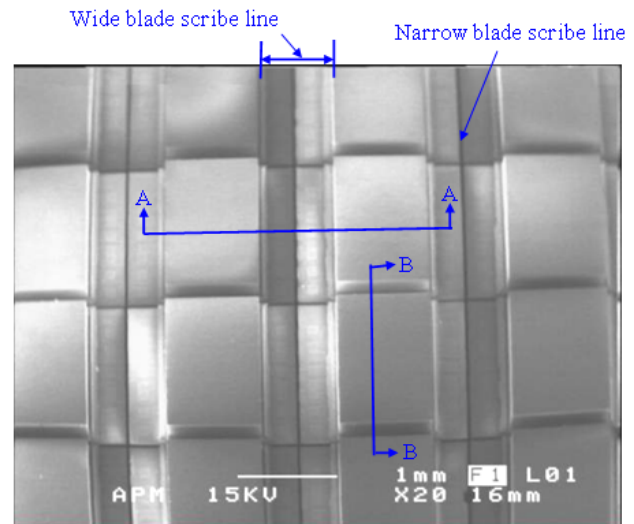
(a)

(b)

Figure 6. Top view of microcapped FBAR filters: (*a*) the whole 6 inch wafer, (*b*) close-up photo.

(a)

(b)

Figure 7. Fabrication results of FBAR filters: (*a*) close-up SEM photo, (*b*) cross-section view.
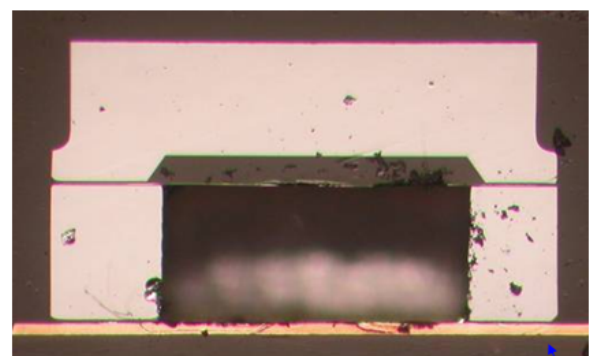
and narrow blades. The cross section *AA* is associated with that illustrated in figure 2. Figure 7(*b*) shows the cross section *BB* (indicated in figure 7(*a*)) of the packaged FBAR device. The microcap cavity had a trapezoid shape resulting from the anisotropic bulk silicon etching. On the other hand, the FBAR cavity had a vertical side wall due to the ICP dry etching process. Figure 7(*b*) also shows that the FBAR cavity is on top of a PCB substrate. After wire-bonding, the FBAR filter would have input/output pins located at the bottom layer of the PCB, as indicated in figure 2(*e*).

The bonding strength is commonly judged by splitting two wafers apart and then observing the bonding surface. Figure 8(*a*) shows the SEM photo of a typical broken silicon wafer after split test on a eutectic-bonded specimen. It is obtained that part of the damaged region was at the silicon substrate, and a very rough surface inside the ring can be observed. Moreover, the shape of the bonding ring is also clearly observed. As shown in figure 8(*b*), the failure point is under the surface of the silicon substrate. At the same time, the cap wafer was destroyed because of the large spilt force. This result demonstrated that the eutectic-bonding technique ensured a high bonding strength of the microcap and FBAR wafer. However, the eutectic-bonded wafers had some yield loss after the subsequent dicing process.

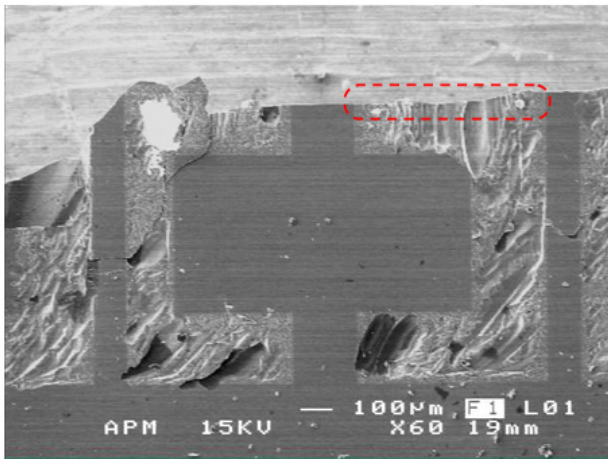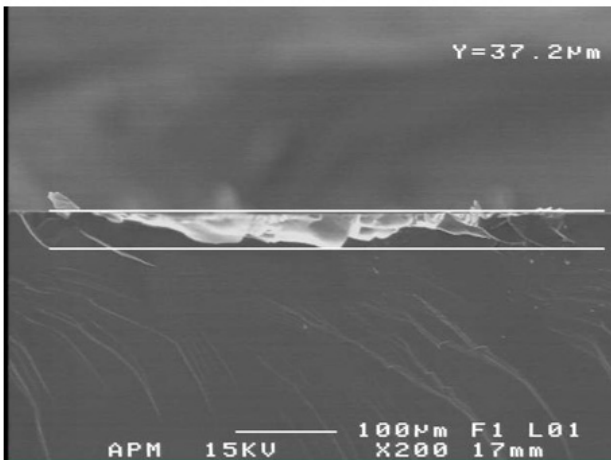The alternative bonding approach was adhesive bonding. The bonding strength of the BCB bonded specimen was measured using a tensile test. There were 28 bonding rings on the specimen; hence, the effective bonding area of this specimen was 25.3×10^6 μm^2. During the tensile test, the top surface of the cap wafer and the bottom surface of the device wafer were adhered to the fixture of the tensile test machine by a commercial adhesive. When the tensile force increased to 56 kgf, fracture occurred at the BCB bonding ring interface. Figure 9 shows the result of the tensile test. Thus, the bonding strength of this specimen was more than 21 MPa. Moreover, this study had employed the IR inspection method to confirm the bonding quality of the eutectic-bonded specimen. According to the IR inspection, this approach had a good bonding quality since the bonding interface had no bubble. In short, both eutectic- and adhesive-bonding methods were capable of providing an acceptable bonding strength for the microcap wafer and the FBAR filter wafer.

To ensure that the temperature and external forces during the bonding process did not change the characteristics of FBAR devices, the adhesive-bonded filter was measured after the microcap process. The dashed line and the solid line in figure 10 depict the performances of the FBAR filter before and after the microcap process, respectively. The measurement results were determined using a probe station and a vector network analyzer. Figure 10(*a*) indicates that the out-of-band performance had nearly no difference. However, some

(a)

(b)

Figure 8. Evaluation of the Au-Si eutectic bonding strength by splitting wafer and SEM observation: (a) top view, (b) cross-section view.

(a)

(b)

Figure 10. Measurement results of a typical microcapped filter: (a) wide band, (b) narrow band. The dashed line represents the filter before the microcap process, and the solid line represents the filter after the microcap process.
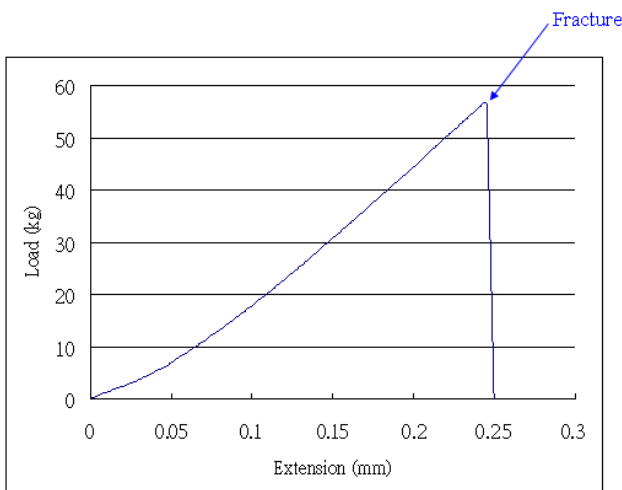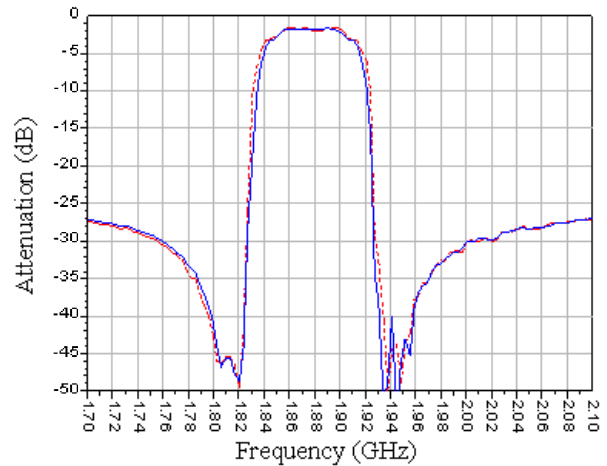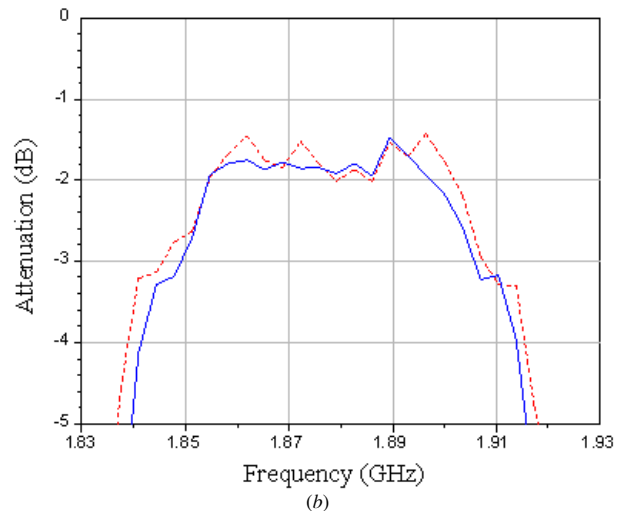

Figure 9. Tensile test result for BCB bonded wafers.

deviations were observed after zooming in to the pass-band region, as shown in figure 10(b). The bandwidth shrank by about 10 MHz and the insertion loss dropped by about 0.2 dB on average. Although the performance of FBAR filters was slightly altered after the microcap processes, the difference was

so small that it can be ignored in practical use. According to the specifications of a PCS filter, the pass-band should range from 1850 MHz to 1910 MHz and the insertion loss must be less than 3.5 dB. In summary, whether the FBAR was microcapped or not, the measured performance fulfilled the specifications of a PCS filter.

The variation of the frequency response with the ambient temperature was also characterized after the microcap process. In addition to the probe station and vector network analyzer, this experiment also employed a thermal chuck to control the ambient temperature during test. The chuck and testing sample were placed inside a testing chamber, so that the ambient temperature could be well controlled. The FBAR filter performance was measured at temperatures varying from $-30\,^{\circ}$C to $85\,^{\circ}$C. The dashed line and the solid line in figure 11 depict the performances of the adhesive-bonded FBAR filter operated at $-30\,^{\circ}$C and $85\,^{\circ}$C, respectively. When temperatures increased from $-30\,^{\circ}$C to $85\,^{\circ}$C, the frequency response of the filter dropped by about 5 MHz, and the insertion loss also dropped by about 0.4 dB. Thus, the temperature coefficient of the frequency was determined as -23 ppm $^{\circ}$C^{-1}. These results were similar to the unpackaged filters. The major
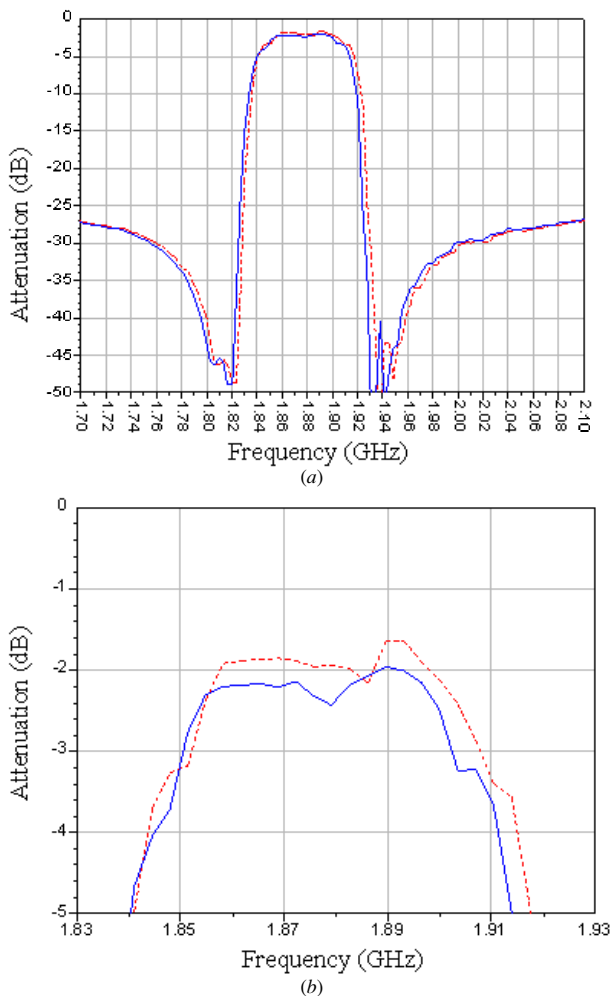
the microcap process were also inspected. The measurement result was verified to meet commercial specifications from $-35\,°C$ to $85\,°C$. The deviation of filter performance after the microcap process was so small that it could be ignored in practice. Therefore, this approach was an effective and economic way for FBAR filter packaging.

Acknowledgment

References

[1] Krishnaswamy S V, Rosenbaum J, Horwitz S, Vale C and Moore R A 1990 Film bulk acoustic wave resonator technology *Proc. IEEE Ultrasonics Symposium (Honolulu, HI, December 1990)* pp 529–36

[2] Park J Y, Lee H C, Lee K H, Lee H M and Ko Y J 2003 Micromachined FBAR RF filters for advanced handset applications, *IEEE Int. Conf. on Solid State Sensors, Actuators and Microsystems (Boston, MA, June 2003)* pp 911–4

[3] Ruby R, Bradley P, Larson J D III and Oshmyansky Y 1999 PCS 1900 MHz duplexer using thin film bulk acoustic resonator (FBARS) *Electron. Lett.* **35** 794–5

[4] Reich H and Grosser V 2001 Overview and development trends in the field of MEMS packaging *14th IEEE Int. Conf. on Micro Electro Mechanical Systems (Interlaken, Switzerland, Jan. 2001)* pp 1–5

[5] Chiang Y-M, Bachman M and Li G P 2004 A wafer-level microcap array to enable high-yield microsystem packaging *IEEE Trans. Adv. Packag.* **27** 490–6

[6] Harpster T J and Najafi K 2003 Field-assisted bonding of glass to Si-Au eutectic solder for packaging applications *16th IEEE Annu. Int. Conf. on Micro Electro Mechanical Systems (Kyoto, Japan, Jan. 2003)* pp 630–3

[7] Cheng Y T, Lin L and Najafi K 2000 Localized silicon fusion and eutectic bonding for MEMS fabrication and packaging *J. Microelectromech. Syst.* **9** 3–7

[8] Oberhammer J, Nikalus F and Stemme G 2003 Selective wafer-level adhesive bonding with benzocyclobutene for fabrication of cavities *Sensors Actuators* A **105** 297–304

[9] Niklaus F, Enoksson P, Kalvesten E and Stemme G 2001 Low-temperature full wafer adhesive bonding *J. Micromech. Microeng.* **11** 100–7

[10] Margomenos A and Katehi L P B 2004 Fabrication and accelerated hermeticity testing of an on-wafer package for RF MEMS *IEEE Trans. Microw. Theory Tech.* **52** 626–36

[11] Feld D and Bradley P 2003 A wafer-level encapsulated FBAR chip molded into a 2.0 mm × 1.6 mm plastic package for use as a PCS full band Tx filter *Proc. 2003 IEEE Ultrasonics Symposium (Honolulu, HI, October 2003)* vol 2 pp 1798–801

[12] Wang K, Frank M, Bradley P, Ruby R and Mueller W 2003 FBAR Rx filters for handset front-end modules with wafer-level packaging *Proc. 2003 IEEE Ultrasonics Symposium (Honolulu, HI, October 2003)* vol 1 pp 162–5

[13] Franosch M, Oppermann K-G, Meches A, Nessler W and Aigner R 2004 Wafer-level-package for bulk acoustic wave (BAW) filters *Microwave Symposium Digest, 2004 IEEE MTT-S International (Fort Worth, TX, June 2004)* vol 2 pp 493–6

[14] Marksteiner S, Handtmann M, Timme H-J, Aigner R, Welzer R, Portmann J and Bauernschmitt U 2003 A miniature BAW duplexer using flip-chip on LTCC *Proc. 2003 IEEE Ultrasonics Symposium (Honolulu, HI, October 2003)* vol 2 pp 1794–7

Figure 11. Temperature stability for a microcapped filter. The dashed line represents the filter measured at $-30\,°C$ and the solid line represents the filter measured at $85\,°C$.

reasons of the frequency shift were expected to be the effect of thermal expansion and the variation of Young's modulus at different temperatures. Similarly, the filter performances were acceptable in practical use, as compared to the specifications of a PCS filter.

4. Conclusions

In this study, the FBAR filter was encapsulated by a microcap using a simple wafer-level packaging process. The present packaging process consists of three steps: bulk etching of silicon wafer, eutectic or adhesive wafer bonding and singulation. These steps are very common for microfabrication. Therefore, this approach provides a promising way to package FBAR filters. Moreover, by using silicon microcaps, the fabricated FBAR filters have a stiff and reliable encapsulation structure. In this study, the measurement on an encapsulated PCS filter has been employed to demonstrate the performance of the present approach. The RF testing confirmed that the filter performance after the microcap process does not alter significantly. Thus, the microcapped FBAR filter fulfilled the specifications of a PCS filter. In addition, temperature characteristics after